Front. Mater. Sci. 2017, 11(3): 271–275
DOI 10.1007/s11706-017-0393-9

RESEARCH ARTICLE

Hydrothermal growth of symmetrical ZnO nanorod arrays on nanosheets for gas sensing applications

Wenyan ZHAO[1], Chuanjin TIAN (✉)[1], Zhipeng XIE[2], Changan WANG[2], Wuyou FU[3], and Haibin YANG[3]

1 School of Materials Science and Engineering, Jingdezhen Ceramic Institute, Jingdezhen 333403, China
2 State Key Laboratory of New Ceramics and Fine Processing, School of Materials Science and Engineering, Tsinghua University, Beijing 100084, China
3 State Key Laboratory of Superhard Materials, Jilin University, Changchun 130012, China

ABSTRACT: The hierarchical ZnO nanostructures with 2-fold symmetrical nanorod arrays on zinc aluminum carbonate ($ZnAl\text{-}CO_3$) nanosheets have been successfully synthesized through a two-step hydrothermal process. The primary nanosheets, which serve as the lattice-matched substrate for the self-assembly nanorod arrays at the second-step of the hydrothermal route, have been synthesized by using a template of anodic aluminum oxide (AAO). The as-prepared samples were characterized by XRD, FESEM, TEM and SAED. The nanorods have a diameter of about 100 nm and a length of about 2 μm. A growth mechanism was proposed according to the experimental results. The gas sensor fabricated from ZnO nanorod arrays showed a high sensitivity to ethanol at 230°C. In addition, the response mechanism of the sensors has also been discussed according to the transient response of the gas sensors.

KEYWORDS: ZnO nanorods; hydrothermal growth; gas sensitivity

Contents

1 Introduction

As a wide-band-gap (3.37 eV) and large exciton-binding energy (60 meV) semiconductor [1–2] ZnO has shown specific electrical properties, optoelectronic properties, gas sensitivity, and electrochemical hydrogen storage ability [3–7]. Among numerous ZnO nanostructures, one-dimensional (1D) nanomaterials, such as nanowires, nanorods, nanobelts, and nanotubes [8–11], have exhibited interesting and particular properties and have been applied as building blocks for the integration of the next generation of photodetectors, nanoelectronics [12], optical devices [13], biosensors [14], solar cells [15], industrial catalysts [16], field-effect transistors [17], and so forth. High-quality nanostructure arrays are not only desirable for industrial application, but also for potential materials to build useful blocks. Nowadays, great progress has been achieved in the synthesis of 1D ZnO nanoarrays through a variety of chemical techniques, including chemical vapor deposition

Received June 26, 2017; accepted July 25, 2017

E-mail: tianchuanjin@jci.edu.cn

(CVD) methods [18], electrochemical deposition methods [19], Langmuir–Blodgett technique [20], and so on. However, the above reaction methods, although successful in some respects, still have their respective limitations and provide room for improvement, especially for achieving the hierarchical ZnO nanorods. Considering the advantages of low cost, environmental friendliness and avoidance of complicated processes and special instruments, in this paper the hydrothermal method is selected to synthesize the hierarchical ZnO nanostructures with 2-fold symmetrical nanorod arrays on zinc aluminum carbonate ($ZnAl\text{-}CO_3$) nanosheets. The possible growth mechanism of the hierarchical ZnO nanorods is also proposed. This preparation method opens a brand new field for synthesizing the similar hierarchical hetero-nanostructures of other complex systems.

Moreover, ZnO is one of the earliest-discovered and well-established gas sensing oxides, which has been extensively studied for detection of inflammable and toxic gases, such as H_2 [21], CO [22], H_2S [23], and NO_2 [24]. However, ethanol gas-sensing properties of the ZnO nanorods had been fewer reported relatively.

Here we report a novel hierarchical ZnO nanostructures which are grown from $ZnAl\text{-}CO_3$ carbonate ($ZnAl\text{-}CO_3$) nanosheets and its ethanol sensitive properties have also been studies. The results show the symmetrical ZnO nanorod arrays present a high sensitivity to ethanol and the possible mechanism is also discussed.

2 Experimental

All of the reagents (analytical grade purity) were purchased from Shanghai Chemical Reagents Co. and were used without further purification. The porous anodic alumina oxide (AAO) with the thickness about 4 μm and pore diameter of 40 nm was prepared, which was similar to the reported in Ref. [25]. In order to obtain the nanosheets on AAO, 0.23 g zinc acetate were dissolved in 70 mL distilled water and the pH was adjusted to 10 using ammonium hydroxide. Then the mixed solution was transferred into a 100 mL Teflon-lined stainless steel autoclave, in which the pretreated AAO was fixed vertically. The hydrothermal treatments were carried out at 90ºC for 5 h. After cooled down naturally, the substrate was washed with deionized water and ethanol, and later dried at 60ºC for 1 h.

The second step of the hydrothermal synthesis was similar to the above process. In an optimized procedure, 0.015 mol/L zinc acetate aqueous solution was added dropwise into the ammonia whilst stirring to turn clear. The hydrothermal process was held at 95ºC for 4 h. After cooled down to room temperature naturally, the substrate was cleaned with deionized water and ethanol, and later dried at 60ºC for 1 h.

The crystal structure and morphology of the samples were characterized by X-ray diffraction (XRD, Rigaku D/max-Ra) with Cu Kα, λ = 0.15418 nm, field emission scanning electron microscopy (FESEM, JEOL JSM-6700F), transmission electron microscopy (TEM, HITACHI H-8100, operated at 200 kV) and selected area electron diffraction (SAED, the TEM attachment).

To fabricate the electrodes for gas sensing measurements, interdigital Au electrodes were deposited on the ZnO nanostructures by sputtering using a shadow mask. The pattern was generated by etching with a patterned photoresist mask. The electrodes consist of four pairs of fingers along with a 20 μm gap. The resistance of the sensor was measured in dry air and in sample gases by a RQ1 intelligent test meter (Qingdao, China). The sensitivity is defined as $S = R_a/R_g$, where R_a and R_g are the resistances of the film in air and in target gas, respectively.

3 Results and discussion

In Fig. 1, Curve a shows the XRD pattern of the AAO template and Curves b and c show the transformation of crystal phases after different steps of the hydrothermal process. After the first hydrothermal growth, the new appeared diffraction peaks are due to the rhombohedral phase of $ZnAl\text{-}CO_3$ [25], which is fabricated easily in the

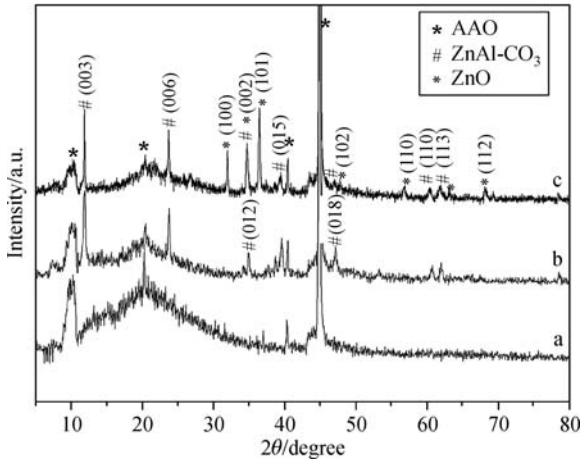

Fig. 1 XRD patterns of the AAO template (a), $ZnAl\text{-}CO_3$ nanosheets (b), and ZnO nanorods on $ZnAl\text{-}CO_3$ nanosheets (c).

alkali hydrothermal environment and exhibits the morphology of hydrotalcite-like hexagonal sheets. After the second step of the hydrothermal synthesis, without regard to the ZnAl-CO_3 peaks, the remainders can be indexed to the hexagonal wurtzite ZnO, and the rather stronger (002) peak reveals the *c*-plane oriented growth.

Figure 2(a) shows the FESEM image of the AAO with plenty of uniform pores with diameters of about 40 nm. After 5 h of hydrothermal disposal, densely packed ZnAl-CO_3 nanosheets have been found on AAO with a uniform size of around 4 μm, as shown in Fig. 2(b). Then, we can deduce that the thickness of ZnAl-CO_3 nanosheets of the sample is about 4 μm. The TEM image and corresponding SAED pattern of one ZnAl-CO_3 nanosheet are shown in Fig. 2(c), which exhibits the hexagonal morphology of single crystal sheet. In order to compare with the optimized time for the morphologies of the product, hydrothermal synthesis of 2 and 4 h are also achieved. Figures 2(d) and 2 (e) display FESEM images of the ZnO nanorods grown at different moments of the second-step of the hydrothermal synthesis. It can be seen from Fig. 2(d) that the ZnO nanorods arise from the nanosheet vertically, and the inset of Fig. 2(d) illustrates an enlarged FESEM image of the vertical ZnO nanorod arrays. It indicates that the ZnO nanorods have self-assembled and oriented with their growth axis perpendicular to the nanosheets. Increasing the reaction time to 4 h while keeping other parameters unchanged, the ZnO nanorods, with uniform diameters (~100 nm) and lengths (~2 μm), pack intimately on the nanosheets, which is shown in Fig. 2(e). The corresponding SAED pattern is shown in the inset of Fig. 2(e), which clearly indicates that the nanorod is single crystal grown along the [001] direction.

The possible formation mechanism can be illustrated as follows: First, ZnAl-CO_3 nanosheets are formed after the first-step of the hydrothermal process [26], which can provide a lattice-matched substrate for the nucleation of ZnO nanorods. At the second-step of the hydrothermal process, the alkaline precursor is substituted by ammonia, which cannot provide the essential concentration of CO_3^{2-} for the formation of ZnAl-CO_3. The high concentration of OH^- ions allows $Zn(OH)_4^{2-}$ to be prior nucleation homogeneously and form ZnO nanorods on the ZnAl-CO_3 surface. Therefore, the self-assembled ZnO nanorod arrays are formed by the homogeneous nucleation and oriented in preferential growth along the [001] direction. The possible chemical reactions occur in the solution are as follows [26]:

$$Zn^{2+} + 4OH^- \rightarrow Zn(OH)_4^{2-} \tag{1}$$

$$Al^{3+} + 4OH^- \rightarrow Al(OH)_4^- \tag{2}$$

$$(1-x)Zn(OH)_4^{2-} + xAl(OH)_4^- + (x/2)CO_3^{2-} + mH_2O \rightarrow [Zn_{1-x}Al_x(OH)_2]^{x+}(x/2)CO_3^{2-}\cdot mH_2O + 2OH^- \tag{3}$$

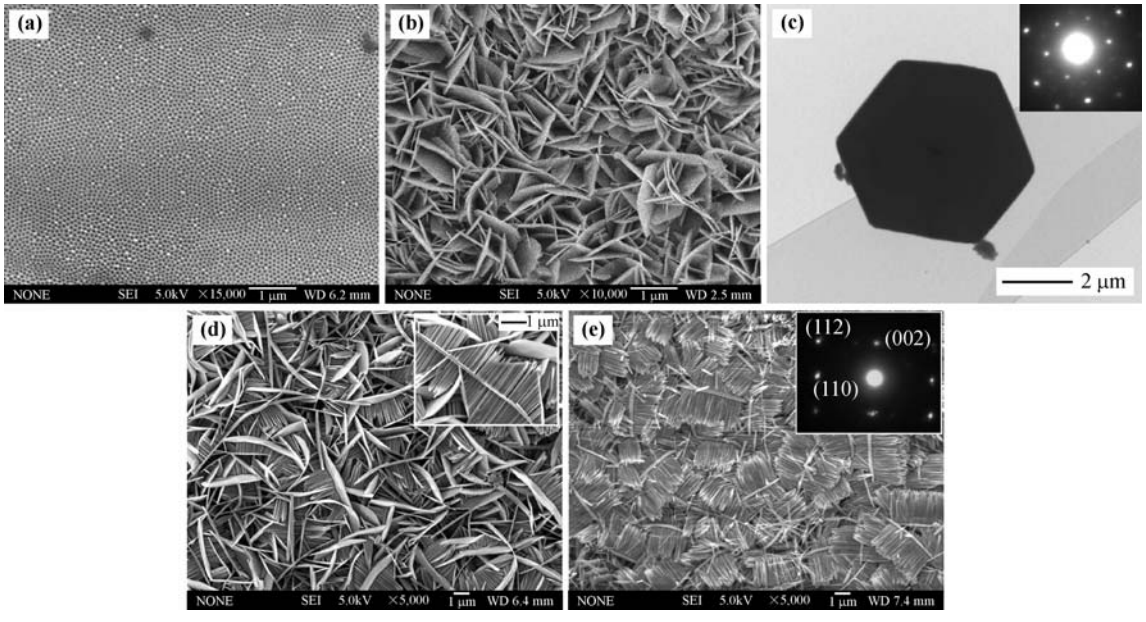

Fig. 2 **(a)** FESEM image of the AAO. **(b)** FESEM and **(c)** TEM images of ZnAl-CO_3 nanosheets after the first-step hydrothermal synthesis, with the SAED pattern shown in the inset. ZnO nanorod arrays on nanosheets after the second-step of the hydrothermal synthesis of **(d)** 2 h and **(e)** 4 h (the insets in (d) and (e) are an enlarged FESEM image and a SAED image of the nanorod, respectively).

$$OH^-_{surface} + OH^-_{soln} + Zn^{2+} \rightarrow ZnO + H_2O \quad (4)$$

The sensitive characteristics of the sensor based on the 2-fold hierarchical ZnO nanostructure films are shown in Fig. 3. In order to find the optimal operating condition, the sensor response at different operating temperatures is tested, and the results are shown in Fig. 3(a). The repeatability of the sensitive properties of all samples are good. Here, the concentration of ethanol is set to 50 ppm (1 ppm = 10^{-6}). It can be seen that the sensor based on ZnO films show different sensitivities within the operating temperatures, and the highest sensitivity is obtained at the operating temperature of 230ºC, and other sensing performances below are exhibited at this operating temperature.

Figure 3(b) shows the sensor response versus time for ethanol from 10 to 1000 ppm. The sensitivity is 2.7 for 10 ppm ethanol, and rises up to 9.4 for 50 ppm and 17.3 for 100 ppm ethanol. The inset of Fig. 3(b) shows the sensitivity of the sensor versus ethanol concentration. The sensitivity increases linearly with increasing the ethanol concentration to 500 ppm. This indicates that the sensor is very suitable for the detection of low concentration ethanol.

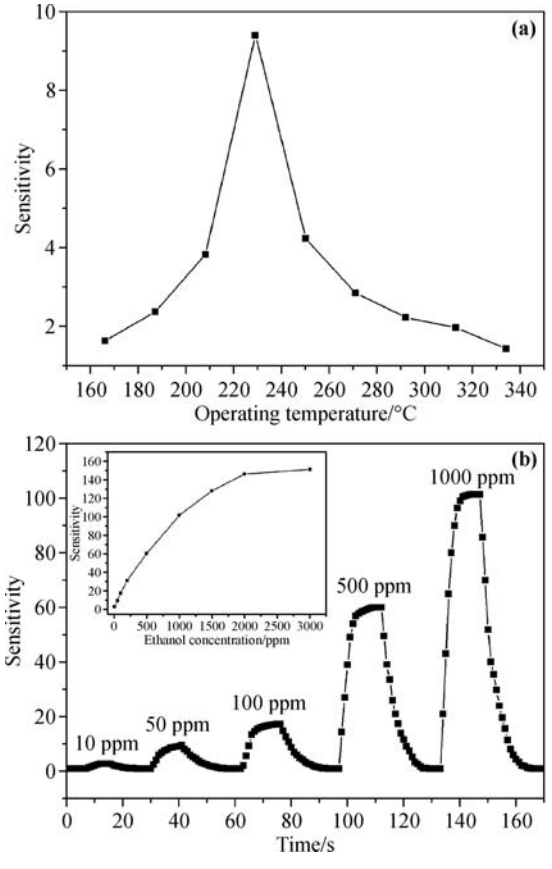

Fig. 3 **(a)** The operating temperature dependence of the sensitivity to 50 ppm ethanol. **(b)** The ethanol concentration dependence of the sensor response (the inset reveals the ethanol concentration dependence of the sensitivity).

A possible mechanism for the ethanol sensing properties in the present study is depicted as follows. It is well known that the change in the resistance of the ZnO gas sensors is primarily caused by the adsorption and desorption of the gas molecules on the surface of the sensing film [18]. In air environment, oxygen molecules will adsorb on the ZnO surface to generate chemisorbed oxygen species (O_2^-, O^{2-}, O^-) and hence decrease the electron concentration, which will cause the ZnO sensing films to show a high resistance. When the reductive ethanol gas is introduced at moderate temperature and subsequently reacts with the oxygen species on the ZnO surface, the concentration of oxygen species will reduce and thus the electron concentration will increase, which eventually increases the conductivity of the ZnO.

4 Conclusions

In summary, single crystalline ZnO nanostructures with hierarchical rod-shaped arrays on nanosheets have been successfully synthesized through the two-step hydrothermal route. The nanosheets are about 4 μm in diameter and the uniform nanorods are ~100 nm in diameters and ~2 μm in length. The growth mechanism is also discussed as well. The gas sensor fabricated from ZnO nanorod arrays exhibited excellent gas sensing properties to the ethanol. The results indicate that this special structure of hierarchical ZnO can be used in gas sensors for detection of low concentration of ethanol. Furthermore, this synthesis method can be used in the fabrication of ZnO-doped semiconductor composites or other semiconductors with novel morphologies.

Acknowledgements This work was financially supported by the National Natural Science Foundation of China (Grant Nos. 51302118 and 11304131), the Science Foundation of the Education Department of Jiangxi Province (No. GJJ13619), Science Foundation of Jiangxi Provincial Department of Science and Technology (No. 20142BAB212006), Jingdezhen Municipal Science and Technology Bureau (103037201), Open Topics of the State Key Laboratory of Super-hard Materials in Jilin University (201313) and the State Key Laboratory of New Ceramics and Fine Processing in Tsinghua University (KF1211, KF201206).

References

[1] Özgür Ü, Alivov Y I, Liu C, et al. A comprehensive review of ZnO materials and devices. Journal of Applied Physics, 2005, 98(4):

041301

[2] Kochuveedu S T, Oh J H, Do Y R, et al. Surface-plasmon-enhanced band emission of ZnO nanoflowers decorated with Au nanoparticles. Chemistry, 2012, 18(24): 7467–7472

[3] Martha S, Reddy K H, Parida K M. Fabrication of In_2O_3 modified ZnO for enhancing stability, optical behavior, electronic properties and photocatalytic activity for hydrogen production under visible light. Journal of Materials Chemistry A: Materials for Energy and Sustainability, 2014, 2(10): 3621–3631

[4] Hu W, Li Z, Yang J. Electronic and optical properties of graphene and graphitic ZnO nanocomposite structures. The Journal of Chemical Physics, 2013, 138(12): 124706

[5] Liu Z, Wang Y, Wang B, et al. PEC electrode of ZnO nanorods sensitized by CdS with different size and its photoelectric properties. International Journal of Hydrogen Energy, 2013, 38 (25): 10226–10234

[6] Wang D, Chu X, Gong M. Hydrothermal growth of ZnO nanoscrewdrivers and their gas sensing properties. Nanotechnology, 2007, 18(18): 185601

[7] Shi L, Naik A J T, Goodall J B M, et al. Highly sensitive ZnO nanorod- and nanoprism-based NO_2 gas sensors: size and shape control using a continuous hydrothermal pilot plant. Langmuir, 2013, 29(33): 10603–10609

[8] Pacholski C, Kornowski A, Weller H. Selbstorganisation von ZnO: von nanopartikeln zu nanostäbchen. Angewandte Chemie, 2002, 114(7): 1234–1237

[9] Wang W Z, Zeng B Q, Yang J, et al. Aligned ultralong ZnO nanobelts and their enhanced field emission. Advanced Materials, 2006, 18(24): 3275–3278

[10] Xia Y, Yang P. Guest editorial: chemistry and physics of nanowires. Advanced Materials, 2003, 15(5): 351–352

[11] Martinson A B F, Elam J W, Hupp J T, et al. ZnO nanotube based dye-sensitized solar cells. Nano Letters, 2007, 7(8): 2183–2187

[12] Hu L, Yan J, Liao M, et al. An optimized ultraviolet-A light photodetector with wide-range photoresponse based on ZnS/ZnO biaxial nanobelt. Advanced Materials, 2012, 24(17): 2305–2309

[13] Wang X, Song J, Wang Z L. Nanowire and nanobelt arrays of zinc oxide from synthesis to properties and to novel devices. Journal of Materials Chemistry, 2007, 17(8): 711–720

[14] Huang X J, Choi Y K. Chemical sensors based on nanostructured materials. Sensors and Actuators B: Chemical, 2007, 122(2): 659–671

[15] Greene L E, Law M, Tan D H, et al. General route to vertical ZnO nanowire arrays using textured ZnO seeds. Nano Letters, 2005, 5 (7): 1231–1236

[16] Chakrabarti S, Dutta B K. Photocatalytic degradation of model textile dyes in wastewater using ZnO as semiconductor catalyst. Journal of Hazardous Materials, 2004, 112(3): 269–278

[17] Fang X, Yan J, Hu L, et al. Thin SnO_2 nanowires with uniform diameter as excellent field emitters: a stability of more than 2400 minutes. Advanced Functional Materials, 2012, 22(8): 1613–1622

[18] Xiang B, Wang P, Zhang X, et al. Rational synthesis of p-type zinc oxide nanowire arrays using simple chemical vapor deposition. Nano Letters, 2007, 7(2): 323–328

[19] Yin Z, Wu S, Zhou X, et al. Electrochemical deposition of ZnO nanorods on transparent reduced graphene oxide electrodes for hybrid solar cells. Small, 2010, 6(2): 307–312

[20] Whang D, Jin S, Wu Y, et al. Large-scale hierarchical organization of nanowire arrays for integrated nanosystems. Nano Letters, 2003, 3(9): 1255–1259

[21] Basu S, Dutta A. Modified heterojunction based on zinc oxide thin film for hydrogen gas-sensor application. Sensors and Actuators B: Chemical, 1994, 22(2): 83–87

[22] Gong H, Hu J Q, Wang J H, et al. Nano-crystalline Cu-doped ZnO thin film gas sensor for CO. Sensors and Actuators B: Chemical, 2006, 115(1): 247–251

[23] Kim J, Yong K. Mechanism study of ZnO nanorod-bundle sensors for H_2S gas sensing. The Journal of Physical Chemistry C, 2011, 115(15): 7218–7224

[24] Baratto C, Sberveglieri G, Onischuk A, et al. Low temperature selective NO_2 sensors by nanostructured fibres of ZnO. Sensors and Actuators B: Chemical, 2004, 100(1–2): 261–265

[25] Sander M S, Gronsky R, Sands T, et al. Structure of bismuth telluride nanowire arrays fabricated by electrodeposition into porous anodic alumina templates. Chemistry of Materials, 2003, 15(1): 335–339

[26] Koh Y W, Lin M, Tan C K, et al. Self-assembly and selected area growth of zinc oxide nanorods on any surface promoted by an aluminum precoat. The Journal of Physical Chemistry B, 2004, 108(31): 11419–11425